THE JOURNAL OF BIOLOGICAL CHEMISTRY VOL. 284, NO. 37, pp. 25230–25240, September 11, 2009

Molecular Regulation of Matrix Extracellular Phosphoglycoprotein Expression by Bone Morphogenetic Protein-2*[S]

Received for publication, April 17, 2009, and in revised form, June 17, 2009 Published, JBC Papers in Press, July 18, 2009, DOI 10.1074/jbc.M109.008391

Young-Dan Cho[‡], Won-Joon Yoon[‡], Kyung-Mi Woo[‡], Jeong-Hwa Baek[‡], Gene Lee[§], Je-Yoel Cho[¶], and Hyun-Mo Ryoo[‡1]

From the Departments of [‡]Cell and Developmental Biology and [§]Biochemistry, School of Dentistry and Dental Research Institute, BK21 Program, Seoul National University, Seoul 110-749 and the [¶]Department of Biochemistry, School of Dentistry and Skeletal Diseases Genome Research Center, Kyungpook National University, Daegu 700-422, Korea

Matrix extracellular phosphoglycoprotein (MEPE) is mainly expressed in mineralizing tissues, and its C-terminal proteolytic cleavage product is an acidic-serine-asparate-rich-MEPE-associated motif (ASARM) that is a strong regulator of body phosphate metabolism and mineralization. There is sufficient data supporting a role for MEPE protein function in mineralization, however, little is known about the regulation of *MEPE* gene expression. As bone morphogenetic protein-2 (BMP-2) is one of the most important signals for calvarial mineralization and *MEPE* expression is higher in mineralized tissues, we attempted to uncover a regulatory circuit between BMP-2 and *MEPE* expression. *Mepe* expression is very low in proliferating MC3T3-E1 cells, but is dramatically increased in the mineralization stage and is strongly stimulated by treatment with BMP-2, even in proliferating cells. Overexpression and knockdown experiments of Smads, Dlx5, and Runx2 indicated that they are indispensable mediators of BMP-2-induced *Mepe* expression. In contrast, Msx2 showed strong inhibition of *Mepe* transcription. PHEX is an enzyme that prevents the release of the ASARM motif, a mineralization inhibitor, from the MEPE molecule. Thus, the MEPE/PHEX ratio may be a good indicator of mineralization progression because we found that the mRNA ratio and protein levels were low when osteoblasts were actively differentiating to the mineralization stage and the ratio was high when the cells reached the mineralization stage when it is assumed that osteocytes may protect themselves and make a space to survive from the mineralized matrix by releasing the ASARM motif. Collectively, *MEPE* expression is bone cell-specific and induced by the BMP-2 signaling pathway. In addition, the MEPE/PHEX ratio of the cell could be a very important barometer indicating the progression of tissue mineralization.

Mineral homeostasis in the body is critical for healthy bones and teeth, and is generally regulated by the calcium-phosphate balance in the bone and kidney networks. In the past, the vitamin D/parathyroid hormone axis was assumed to be a single major circuit in bone-renal phosphate regulation, but recently, new bone-renal phosphate regulating factors have been identified. The finding of fibroblast growth factor 23 (FGF23),[2] phosphate-regulating genes with homologies to endopeptidases on the X chromosome (PHEX) and matrix extracellular phosphoglycoprotein (MEPE) genes, and their pathophysiological roles in the genetic diseases of mineral metabolism, have provided a great deal of insight into the understanding of bone- and mineral-related diseases. Among these, autosomal-dominant hypophosphatemic rickets (OMIM number 193100) is characterized by renal phosphate wasting, hypophosphatemia, and inappropriately normal 1,25-dihydroxyvitamin D_3 levels (1). Autosomal-dominant hypophosphatemic rickets is caused by a missense mutation of FGF23, which is resistant to proteolysis by PHEX and increases the half-life of full-length phosphaturic FGF23 (2). Second, X-linked hypophosphatemic rickets (*Hyp*, OMIM number 307800) is characterized by defective renal phosphate handling, aberrant vitamin D metabolism, and defective calcification of bone (3). X-linked hypophosphatemic is caused by an inactivating mutation in PHEX that increases the uncleaved full-length FGF23 and/or abnormal processing of MEPE. Third, oncogenic hypophosphatemic osteomalacia is caused by tumor-expressed proteins, MEPE and/or FGF23, whose overexpression results in abnormal renal phosphate metabolism and bone mineralization. Based on these data, FGF23, PHEX, and MEPE are generally accepted as the main regulators of systemic phosphate levels and tissue mineralization (4).

MEPE is also called osteoblast/osteocyte factor 45 as it is mainly expressed in osteoblasts and osteocytes, and was first identified in a cDNA library of oncogenic hypophosphatemic osteomalacia (5). The *MEPE* gene encodes a 525-amino acid extracellular matrix protein (6). MEPE shares sequence homology with small integrin binding ligand, *N*-linked glycoprotein (SIBLING) family proteins such as bone sialoprotein, dentin

* This work was supported by the Korea Health 21 R&D Project, Ministry of Health and Welfare Project A010252, and a Korea Research Foundation grant funded by Korean Government (MOEHRD) Grant KRF-2006-I00680A.

[S] The on-line version of this article (available at http://www.jbc.org) contains supplemental Figs. S1–S4.

[1] To whom correspondence should be addressed: 28 Yeongeon-dong, Jongno-gu, Seoul 110-749, Korea. Tel.: 82-2-740-8743; Fax: 82-2-741-1959; E-mail: hmryoo@snu.ac.kr.

[2] The abbreviations used are: FGF23, fibroblast growth factor 23; PHEX, phosphate-regulating genes with homologies to endopeptidases on the X chromosome; MEPE, matrix extracellular phosphoglycoprotein; FBS, fetal bovine serum; α-MEM, α-minimal essential medium; HA, hemagglutinin; EMSA, electrophoretic mobility shift assay; ChIP, chromatin immunoprecipitation; WT, wild-type; MT, mutant; *Gapdh*, glyceraldehyde-3-phosphate dehydrogenase; siRNA, small interfering RNA; *Alp*, alkaline phosphatase.

sialophosphoprotein, osteopontin, and the dentin matrix protein, all of which are clustered on chromosome 4q21 in humans and 5q in mouse (5, 7). Two functional domains of MEPE have been well defined; one is the centrally located motif that includes an RGD, cell adhesion domain, and a SGDG, glycosaminoglycan (GAG) interaction domain. AC-100, a 23-amino acid synthetic peptide comprised of RGD and SGDG, has demonstrated strong osteogenic activity (8, 9). The other domain is a C-terminal ASARM motif that is common among the SIBLING family proteins although they are not functionally conserved (10). The C-terminal ASARM motif of the MEPE protein can be cleaved by proteolytic activity of cathepsin B and the proteolytic cleavage is protected by another enzyme, PHEX (4). The released ASARM motif circulates in the bloodstream to regulate reabsorption of phosphate in the renal proximal tubules and mineralization in bones and teeth (4, 11). For this reason, the ASARM peptide is also called minhibin due to its bone mineralization-inhibiting action, and phosphatonin by its phosphate reabsorption-inhibiting action. The targeted disruption of the *MEPE* gene in mice showed strongly increased bone mass that is not due to decreased osteoclastic activity but, rather, increased osteoblastic activity (12). On the other hand, overexpression of MEPE in bone cells decreases the bone mass and high phosphate diet-induced renal stone development (13). The results from mouse genetic studies indicate that the function of the whole MEPE molecule is primarily due to the function of the C-terminal ASARM peptide.

Despite advances in our understanding of MEPE function, the molecular mechanism regulating the expression of *MEPE* has not yet been investigated. Moreover, the transcriptional regulation of other SIBLING family genes has been relatively well described, however, that of *MEPE* has not been reported (14). Because MEPE controls the mineralization of both hard and soft tissues, understanding how its expression is regulated will provide great insight into target selection for the modulation of biomineralization. Previously we have compared expressed mRNAs between developing mouse calvariae and sutural mesenchyme by microarray analysis (15). We found that *Mepe* is one of the most highly expressed genes in mineralizing tissue. And it is well known that *Mepe* expression is specific in the bone (12, 24). In addition, we have also reported that BMP-2 and its downstream transcription factors, Dlx5 and Runx2-II, are specifically expressed in mineralizing calvarial tissue, but not in sutural mesenchyme (16). Based on the common expression patterns of BMP-2 signaling molecules and *Mepe*, we can assume that BMP-2 signaling regulates *Mepe* expression in bone cells. In this study, we demonstrate for the first time how BMP-2 signaling and its downstream transcription factors regulate *Mepe* gene transcription.

EXPERIMENTAL PROCEDURES

Cell Culture—Mouse myogenic C2C12 cells and rat osteosarcoma cell line ROS 17/2.8 cells were maintained in Dulbecco's modified Eagle's medium (Hyclone, Logan, UT) with 10% fetal bovine serum (FBS), and then osteoblast-like MC3T3-E1 cells and Runx2$^{-/-}$ calvarial cell line H1-127-21-2 were maintained in α-MEM with 10% FBS as previously described (16, 17). The osteogenic media includes ascorbic acid (50 μg/ml) and β-glycerophosphate (10 mM) in α-MEM with 10% FBS as previously described (18).

Antibodies—Anti-hemagglutinin (HA) (HA11.3) antibody was purchased from Covance (Princeton, NJ). Horseradish peroxidase-conjugated anti-FLAG (M2) (anti-FLAG-horseradish peroxidase) was purchased from Sigma. Anti-immunoglobulin G (IgG) antibody was purchased from Santa Cruz (Santa Cruz, CA). Anti-Dlx5 antibody was purchased from TaKaRa (TaKaRa Shuzo, Shiga, Japan). Anti-β-actin and -Smad 1/5/8 antibodies were purchased from Abcam (Cambridge, MA), and horseradish peroxidase-conjugated anti-mouse and anti-rabbit secondary antibodies were purchased from Pierce.

Materials—Bioactive recombinant human BMP-2 protein was purchased from R&D Systems (Minneapolis, MN). The Superscript™ first-strand synthesis system for reverse transcription was purchased from Invitrogen. For chromatin immunoprecipitation assays, single-stranded DNA and protein G-agarose beads were purchased from Sigma and Upstate Biotechnology (Charlottesville, VA), respectively. For the radioactive electrophoretic mobility shift assay (EMSA), we purchased [γ-^{32}P]ATP from PerkinElmer Life Sciences and a DNA 5′-end labeling system kit from Promega (Madison, WI). DNA 5′-end labeling and EMSA were performed according to the manufacturer's instructions. The Dlx5 and Msx2 proteins were produced by *in vitro* transcription and translation using the TnT-coupled reticulocyte lysate system (Promega).

DNA Construction—The construction of the Dlx5 (pcDNA3.1-Dlx5) and Runx2 expression vectors have been described previously (17, 19). Dlx5 and Msx2 full-length cDNAs were generated by PCR and subcloned into pcDNA3.1 for HA epitope fusion proteins and pcDNA3 for FLAG (M2) epitope fusion proteins, respectively. All fusion proteins have N-terminal tags and were confirmed by Western blot analysis, previously (20). The mouse *Mepe* promoter (−608 to +256 bp) is based on GenBank™ accession number AF314964. *Mepe* promoter deletion constructs were generated by serial deletion from the 5′-end of the promoter with PCR, and the fragments were ligated into NheI and XhoI sites, respectively. The *Mepe* promoter WT (−608 to +256 bp) and deletion constructs D-270 (−270 to +256 bp), D-160 (−160 to +256 bp), and D-136 (−136 to +256 bp) were cloned into the pGL3-basic vector (Promega) for the luciferase reporter assay. The forward and reverse primers for promoter deletion constructs are listed in Table 1.

Site-directed Mutagenesis of Homeodomain and Runx2 Binding Sites—To produce a construct that bears a mutation in the putative homeodomain binding sites, a site-directed mutagenic PCR was performed with the −253 Mut and −147 Mut oligonucleotides for M-253 and M-147 (see Table 1 for the sequence) and the universal RVprimer3 (RV3) and GLprimer2 (GL2) listed in Table 1. For making a construct that bears a mutation in the putative Runx2 binding sites, a site-directed mutagenic PCR was performed with the −165 Mut and −127 Mut oligonucleotides for M-165 and M-127 (see Table 1 for the sequences) and the universal RVprimer3 (RV3) and GLprimer2 (GL2) listed in Table 1. The PCR products of the promoter mutation were digested with NheI and XhoI, and those were replaced with the wild-type counterpart of the reporter vector.

TABLE 1

Primer sequences for construction of Mepe promoter deletion mutants and site-directed mutagenesis

The boldfaced letters correspond to restriction enzyme sites for NheI (forward primer) or XhoI (reverse primer). The lowercase letters designate the substitution of nucleotide for site-directed mutagenesis.

Name	Oligonucleotide sequence	Sequence Location (bp)
WT (forward)	5′-A**GCTAGC**TCTCGCCATGAGTGCTTCTGTTGA-3′	-608 to -586
-270 Del (forward)	5′-CCC**GCTAGC**TCTAAAAATCAGTTCTAA-3′	-270 to -253
-160 Del (forward)	5′-CCC**GCTAGC**AAAACATTTTTAGATTA-3′	-160 to -143
-136 Del (forward)	5′-AAA**GCTAGC**CATACCCCCTGTG-3′	-136 to -123
WT (reverse)	5′-ATT**CTCGAG**TAGTCAGCTCACAGGC-3′	+256 to +240
-253 Mut (forward)	5′-GTTCTAAAAATCAGTTCTAgcgggTTTGCAACATAATGTCCAAAC-3′	-272 to -228
-253 Mut (reverse)	5′-GTTTGGACATTATGTTGCAAAcccgcTAGAACTGATTTTTAGAAC-3′	-272 to -228
-165 Mut (forward)	5′-GCAGCTTTCCaccttCAAACATTTTTAG-3′	-175 to -158
-165 Mut (reverse)	5′-CTAAAAATGTTTGaaggtGGAAAGCTGC-3′	-175 to -158
-147 Mut (forward)	5′-ACAAAACATTTTTAGgccaAAaccggCATACCCCCTGTGGT-3′	-162 to -122
-147 Mut (reverse)	5′-ACCACAGGGGGTATGccggcTTcggcCTAAAAATGTTTTGT-3′	-162 to -122
-127 Mut (forward)	5′-CCCCtgaacaCATCtggaagcATTTGT-3′	-131 to -115
-127 Mut (reverse)	5′-ACAAATgcttccaGATGtgttcaGGGG-3′	-131 to -115
RV3 (forward)	5′-CTAGCAAAATAGGCTGTCCCCAGTGCAAGTGCA-3′	
GL2 (reverse)	5′-CTTTATGTTTTTGGCGTCTTCCATGGTGGCTTTACC-3′	

Reverse Transcription PCR and Quantitative Real Time PCR—Conventional reverse transcription-PCR for murine *Mepe* and *Phex* was performed with the primers listed in Table 2. Quantitative real time PCR was performed using TaKaRa SYBR premix Ex Taq (Takara, Japan) on a Applied Biosystems 7500 real time PCR system (Foster City, CA). PCR primers were synthesized by Integrated DNA Technology (Coralville, IA). All samples were run in duplicate, and the relative levels of *Mepe* mRNA were normalized to those of glyceraldehyde-3-phosphate dehydrogenase (*Gapdh*). The primer sets for real time PCR are listed in Table 2.

Knockdown Assay with siRNA—To knock down Dlx5, Runx2, and Smad1/5 expression, siRNAs against Dlx5 and Runx2 (si-GENOME SMART pool) were purchased from Dharmacon (Lafayette, CO). The siRNA against Smad1/5 was purchased from Invitrogen (Stealth™/siRNA duplex oligoribonucleotides). siGENOME Non-targeting siRNA-2 was used as a control (scramble siRNA). 60 or 40 pmol of siRNA was transfected by electroporation in MC3T3-E1 cells. After transfection, the cells were cultured for 36 h to 90% confluence and then treated with or without BMP-2 (100 ng/ml) for 24 h.

Transient Transfection—C2C12 and MC3T3-E1 cells were plated in 100-mm plates and cultured up to 90% confluence. After harvesting the cells, a transfection by electroporation was performed using a Microporator (NanoEnTek, MA) with a

TABLE 2

Primer sequences for reverse transcription PCR and quantative real time PCR

Name	Oligonucleotide sequence
MEPE (forward)	5′-GTCTGTTGGACTGCTCCTCTT-3′
MEPE (reverse)	5′-CACCGTGGGATCAGGATACA-3′
PHEX (forward)	5′-GAAAGGGGACCAACCGAGG-3′
PHEX (reverse)	5′-AACTTAGGAGACCTTGACTCACT-3′
Dlx5 (forward)	5′-TCTCTAGGACTGACGCAAACA-3′
Dlx5 (reverse)	5′-GTTACACGCCATAGGGTCGC-3′
Runx2 (forward)	5′-TTCTCCAACCCACGAATGCAC-3′
Runx2 (reverse)	5′-CAGGTACGTGTGGTAGTGAGT-3′
ALP (forward)	5′-GGCTACATTGGTCTTGAGCTTTT-3′
ALP (reverse)	5′-CCAACTCTTTTGTGCCAGAGA-3′
Osteocalcin (forward)	5′-CTGACAAAGCCTTCATGTCCAA-3′
Osteocalcin (reverse)	5′-GCGCCGGAGTCTGTTCACTA-3′
BSP (forward)	5′-CAGGGAGGCAGTGACTCTTC-3′
BSP (reverse)	5′-AGTGTGGAAAGTGTGGCGTT-3′
Type 1 collagen (forward)	5′-GCTCCTCTTAGGGGCCACT-3′
Type 1 collagen (reverse)	5′-CCACGTCTCACCATTGGGG-3′
GAPDH (forward)	5′-GGCCTCACCCCATTTGATGT-3′
GAPDH (reverse)	5′-CATGTTCCAGTATGACTCCACTC-3′

TABLE 3
Primer sequences for ChIP assay

Name	Oligonucleotide sequence
ChIP-h2 (forward)	5′-CCTACTTACACGTATGCAACCCA-3′
ChIP-h2 (reverse)	5′-GCTGCTATCAAATGTTCCAGAAAG-3′
ChIP-h3 (forward)	5′-CTTTCTGGAACATTTGATAGCAGC-3′
ChIP-h3 (reverse)	5′-CTTAGTCTCTGGGCATTTGCTG-3′

10-μl gold tip according to the manufacturer's instructions. ROS 17/2.8 cells were plated in a 96-well assay plate, and after overnight culture the cells were transfected with Hilymax (Dojindo, Japan) according to the manufacturer's instructions. Transfections were performed with 0.5 μg of Dlx5 or Msx2 expression vector or pcDNA3.1 empty vector as a control and 0.15 μg of the *Mepe* promoter luciferase reporter vector. All plasmid DNA was prepared using a DNA Maxi-prep kit (GENOMED, Loehne, Germany). We used Dlx5, Msx2, and Runx2 expression vectors, which were previously described and confirmed by Western blot analysis (16, 17, 20).

Luciferase Reporter Assay—After cells lysis with passive lysis buffer (Promega), luciferase activity was detected using a Bright-Glo™ Luciferase assay system (Promega) with a Glo-Max-Multi Detection System machine (Promega).

EMSA—The sequences of the wild-type and mutant oligonucleotides are listed in Fig. 5*E*. These double-stranded DNA probes were end-labeled with [r-^{32}P]ATP using the DNA 5′-end labeling system (Promega). Dlx5 and Msx2 proteins were produced by *in vitro* transcription and translation using the TNT-coupled reticulocyte lysate (Promega). The Dlx5 and/or Msx2 proteins were incubated with the labeled, double-stranded DNA probes in the presence or absence of a 10-, 50-, and 100-fold molar excess of the unlabeled competitor for 30 min at room temperature. For the Supershift assay, the Dlx5 proteins were preincubated with anti-HA antibody for 30 min at room temperature (we used the Dlx5 expression vector with the HA tag). The protein-DNA complexes were then separated at room temperature on a 5% polyacrylamide gel containing 0.5× TBE buffer.

Chromatin Immunoprecipitation Assays—The chromatin immunoprecipitation (ChIP) assay was performed as previously described (16). Cells were seeded in 100-mm dishes at a density of 1×10^7 cells per dish and then transfected with expression plasmids for FLAG-Msx2 and HA-Dlx5. The PCR primer pairs used to detect DNA segments for the ChIP analysis are listed in Table 3.

Alkaline Phosphatase Staining—Cells were washed twice with phosphate-buffered saline, fixed with 2% paraformaldehyde, and stained for alkaline phosphatase (ALP) according to the manufacturer's instructions (Sigma).

Alizarin Red Staining—Cells were washed twice with phosphate-buffered saline, fixed with 70% ethanol for 1 h, washed twice with distilled water, and stained with 40 mM alizarin red S (Sigma) for 10 min, then washed three times with distilled water.

RESULTS

Mepe Expression Is Bone-specific and Mineralization Stage-specific in Osteoblast Differentiation—Our previous DNA ChIP analysis comparing mRNA expression patterns between mineralizing calvarial bone tissue and unmineralized suture tissue indicated that *Mepe* showed 28-fold higher expression in mineralizing calvarial tissue, and that *Mepe* was one of the top 20 highly expressed genes in calvarial tissue (15). This microarray result was confirmed by conventional reverse transcriptase-PCR (Fig. 1*A*) and quantitative real time PCR analysis in which *Mepe* expression was found to be about 800-fold higher in bone tissue (data not shown). To understand the *Mepe* expression pattern in osteoblast differentiation, a long-term culture of MC3T3-E1 cells in osteogenic medium was performed, as previously described (18). *Mepe* expression increased gradually until day 14 of culture, and then increased abruptly at day 21 when the culture underwent the mineralization process. The expression pattern of the other bone marker genes, especially osteocalcin and bone sialoprotein, clearly showed that the culture had undergone a typical osteoblast differentiation process and that there must have been significant mineralization between days 14 and 21 of the cell culture (Fig. 1*B*), which was verified by ALP and alizarin red staining of the MC3T3-E1 cells (supplemental Fig. S1).

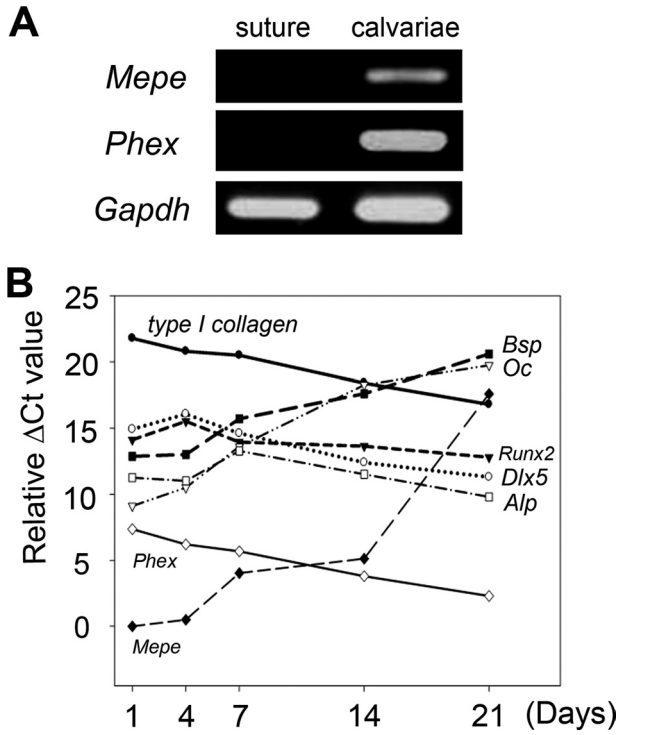

FIGURE 1. ***Mepe* expression is bone cell-specific and increased during osteoblast differentiation.** *A*, *Mepe* and *Phex* expression were determined by conventional reverse transcriptase-PCR using *Gapdh* as an internal control. *B*, MC3T3-E1 cells were cultured for 21 days in the osteogenic media (50 μg/ml ascorbic acid, 10 mM β-glycerophosphate in α-MEM supplemented with 10% FBS). *Mepe*, *Phex*, and other bone marker gene expressions were determined by quantitative real time PCR, and their expression levels presented by the relative ΔCt value. The relative ΔCt value means that the highest ΔCt value of the target genes − each individual ΔCt value (ΔCt = Ct value of a target gene − Ct value of *Gapdh*).

Mepe Expression Is Bone Cell-specific and Induced by BMP-2—Our previous study indicated that BMP-2 is a potent inducer of osteoblast differentiation (21) and calvarial mineralization (16, 19). In addition, BMP R-Smads and Dlx5 are indispensable mediators of BMP-2-induced Runx2-II and alkaline phosphatase expression (17, 22). Because *Mepe* expression is bone cell-

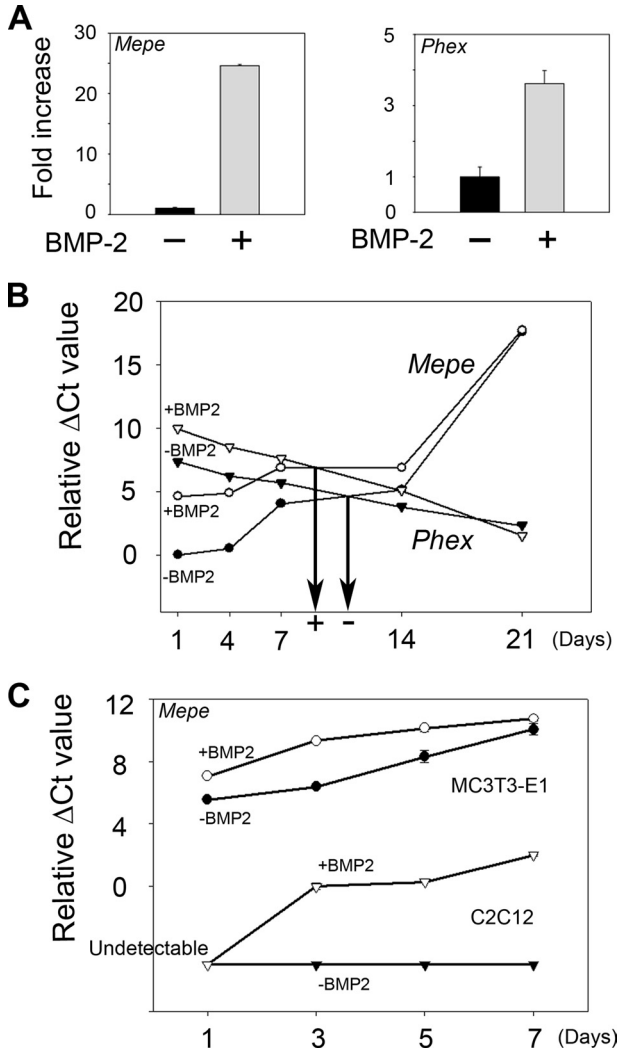

FIGURE 2. ***Mepe* expression is induced by BMP-2 exclusively in the bone cell.** *A*, MC3T3-E1 cells cultured in α-MEM were treated with BMP-2 (100 ng/ml) for 1 day. *Mepe* and *Phex* expression were determined by quantitative real time PCR. *B*, MC3T3-E1 cells were cultured for 21 days in the osteogenic media (α-MEM supplemented with 50 μg/ml ascorbic acid and 10 mM β-glycerophosphate) with (+*BMP2*) or without (−*BMP2*) BMP-2 treatment (100 ng/ml) once for 3 days, and then the medium was changed every 2 to 3 days without additional treatment with BMP-2. Cells were harvested at the indicated time points. *Mepe* and *Phex* expressions were determined by quantitative real time PCR. *Error bars* represent S.D. based on triplicates per each experiment. *C*, C2C12 and MC3T3-E1 cells were cultured for 7 days with (+*BMP2*, 100 ng/ml) or without (−*BMP2*) BMP-2 treatment (100 ng/ml) in Dulbecco's modified Eagle's medium with 5% FBS, and osteogenic media, respectively. *Mepe* expression was determined by quantitative real time PCR. For all quantitative real time PCR data, the relative levels of *Mepe* and *Phex* mRNA were normalized to mRNA levels of glyceraldehyde-3-phosphate dehydrogenase (*Gapdh*) and indicated by the relative ΔCt value.

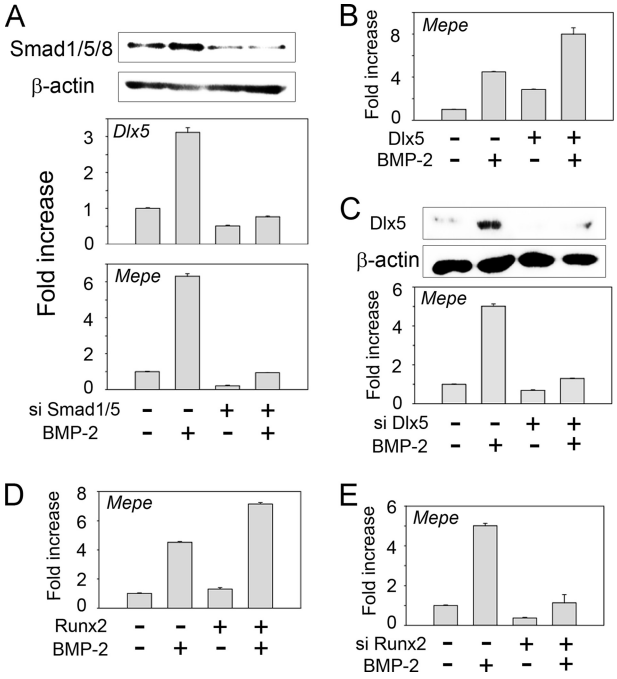

FIGURE 3. ***Mepe* expression is stimulated by BMP-2 signaling.** *A*, MC3T3-E1 cells were transfected by electroporation with 40 pmol of scramble siRNA as a control and siRNA targeted against Smad1/5. After 48 h of transfection, cells were treated with BMP-2 (100 ng/ml) for 24 h. Smad1/5/8 and β-actin were detected by immunoblotting and *Dlx5* and *Mepe* mRNA expressions were determined by quantitative real time PCR and normalized to *Gapdh*. *B*, MC3T3-E1 cells were transfected by electroporation with Dlx5 expression vector or pcDNA3.1 empty vector, and treated with BMP-2 (100 ng/ml) for 24 h. *Mepe* expression was determined by quantitative real time PCR and normalized to *Gapdh*. *C*, MC3T3-E1 cells were transfected by electroporation with 60 pmol of scramble siRNA as a control and siRNA targeted against Dlx5. After 48 h of transfection, cells were treated with 100 ng/ml of BMP-2 for 24 h. Dlx5 and β-actin were detected by immunoblotting and the *Mepe* mRNA level was measured by quantitative real time PCR and normalized to *Gapdh*. *D*, MC3T3-E1 cells were transfected by electroporation with Runx2 expression vector or pcDNA3.1 empty vector, and treated with or without BMP-2 (100 ng/ml) for 24 h. *E*, MC3T3-E1 cells were transfected by electroporation with 60 pmol of scramble siRNA as a control and siRNA targeted against Runx2. After 48 h of transfection, cells were treated with BMP-2 (100 ng/ml) for 24 h. The *Mepe* mRNA level was determined by quantitative reverse transcriptase-PCR and normalized with *Gapdh*. *Error bars* represent S.D. based on triplicates per each experiment.

specific (12, 24) and highly increased in the mineralization stage of osteoblast differentiation, we hypothesized that *Mepe* expression also would be regulated by BMP-2 signaling. *Mepe* expression was dramatically (about 25-fold) increased by treatment of confluent MC3T3-E1 cells with BMP-2 (100 ng/ml). Also, *Phex* expression was increased by BMP-2 treatment (Fig. 2*A*). In the long-term culture of MC3T3-E1 cells, the increase of *Mepe* expression and the decrease of *Phex* expression intersected around day 11 (Fig. 2*B*, *arrow* indicating "−" in the *x* axis). Even if the expression of both genes was commonly stimulated by BMP-2, the intersection point was advanced to day 9 (Fig. 2*B*, *arrow* indicating "+" in the *x* axis). In the case of MC3T3-E1 cells, basal *Mepe* expression was much higher, at least 26-fold higher than in C2C12 cells. However, the basal *Mepe* gene expression in C2C12 cells was not detectable in the 40 cycles of real time PCR. Moreover, even after treatment of BMP-2, the *Mepe* expression level in C2C12 cells was much lower than that in untreated MC3T3-E1 cells (Fig. 2*C*), indicating that gene expression is bone cell-specific. In this culture, the bone marker gene *Alp* expression was increased, whereas myoblast marker gene *MyoD* expression was decreased by BMP-2 (data not shown). BMP-2 treatment in MC3T3-E1 cells increased the level of phosphorylated BMP R-Smads (Smad 1/5/8), which subsequently stimulated *Dlx5* and *Mepe* mRNA levels, as previously demonstrated (17). The knockdown of BMP R-Smads by siRNA treatment clearly indicates that *Dlx5* and *Mepe* are common downstream targets of activated BMP R-Smads (Fig. 3*A*). The overexpression of Dlx5 strongly stimulated *Mepe* mRNA expression, demonstrating an additive effect with BMP-2 treatment (Fig. 3*B*). In contrast, knockdown of

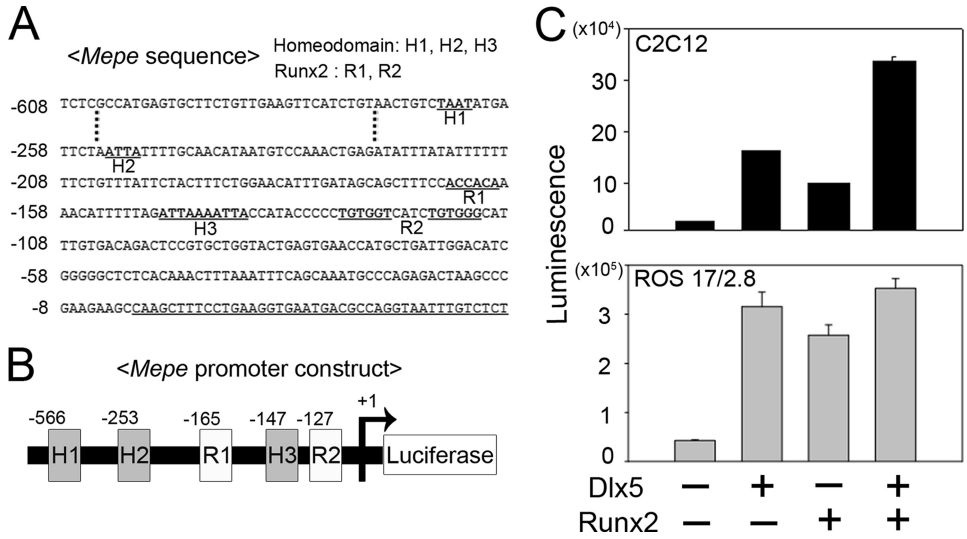

FIGURE 4. ***Mepe* promoter has a homeodomain and Runx2 response elements**. *A*, mouse *Mepe* promoter between −608 and +256 bp has a homeodomain and Runx2 binding sites that are highly conserved among the vertebrate species (human, mouse, and rat). We designated each of the response elements as *H1*, *H2*, and *H3* for homeodomains, *R1* and *R2* for Runx2. *B*, the *Mepe* promoter construct is illustrated in *B*. *C*, C2C12 and ROS 17/2.8 cells were transiently cotransfected with the *Mepe* promoter construct together with the Dlx5 and/or Runx2 expression vectors by electroporation and Hilymax transfection reagent for C2C12 and ROS 17/2.8, respectively. Luciferase activities were determined based on triplicates per each experiment and three independent experiments.

Dlx5 by siRNA dramatically reversed BMP-2-stimulated *Mepe* mRNA expression (Fig. 3*C*).

Runx2 Is Involved in BMP-2-induced Mepe Expression and Has an Additive Effect with Dlx5—Our previous papers (16, 17) indicated that Runx2-II is a downstream target of BMP-2-induced Dlx5 activation. As *Mepe* mRNA levels are increased by BMP-2 treatment and Dlx5 overexpression, we tested whether *Mepe* was also stimulated by the BMP-2 downstream transcription factor Runx2. *Mepe* promoter activity was increased by Dlx5 or Runx2 overexpression in C2C12 and ROS 17/2.8 cells and coexpression of both genes had an additive effect (Fig. 4*C*). In comparison with non-osteogenic C2C12 cells, ROS 17/2.8 cells showed enhanced activity of the *Mepe* promoter activity in response to Runx2, with a much higher basal Dlx5 level. Runx2 overexpression increased *Mepe* mRNA levels (Fig. 3*D*) and knockdown of Runx2 by siRNA significantly suppressed *Mepe* mRNA levels (Fig. 3*E*), as did the knockdown of Dlx5 by siRNA (Fig. 3*C*). These observations suggest that the induction of *Mepe* expression by BMP-2 requires Dlx5 and Runx2 activities.

Dlx5 Specifically Enhances Mepe Gene Transcription—We performed an *in silico* analysis of the *Mepe* proximal promoter between the −608 nucleotide and putative transcription start site (+1), and found three putative homeodomain binding sequences (Fig. 4*A*, designated as *H1*, −566 to −563; *H2*, −253 to −250; *H3*, −147 to −138, respectively, and H3 had two tandem linked putative Dlx5 binding sequences). These three binding sites are well conserved among human, mouse, and rat *MEPE* genes, except for H1, which is not conserved in the rat. The proximal promoter also includes two putative Runx2 binding sequences (Fig. 4*A*, named *R1*, −165 to −160, and *R2*, −127 to −112, with R2 having two consecutive Runx2 binding sequences separated by 4 bp). To confirm the promoter binding affinity for Dlx5, we prepared 5′-serial deletion constructs of the *Mepe* promoter as illustrated in Fig. 5*A*. *Mepe* promoter deletion analysis showed a dramatic decrease in basal reporter activity from WT to D-270 in C2C12 non-bone cells (Fig. 5*B*) and from D-270 to D-160 in ROS 17/2.8 bone cells (Fig. 5*C*). This result shows that an element between D-270 and D-160 is important for *Mepe* transactivation in a bone cell-specific transcriptional context. Interestingly, the basal reporter activity of the full-length promoter was completely recovered by D-136. Dlx5 cotransfection resulted in a 40–100-fold induction in C2C12 cells and a 1.1–1.7-fold induction in ROS 17/2.8 cells, which correlates well with our previous finding that Dlx5 is bone cell-specific (17). In other words, the Dlx5 level in ROS 17/2.8 must be almost saturated, as overexpression of Dlx5 did not cause a significant change. However, in non-bone cell lines like C2C12 premyoblast cells, Dlx5 is not expressed at all so the effect of Dlx5 overexpression is demonstrated clearly. The basal activity changes of *Mepe* promoter deletion constructs in ROS 17/2.8 cells (Fig. 5*C*) and the fold-induction by Dlx5 in C2C12 cells indicate that the 2nd homeodomain binding site (H2) is important for Dlx5-induced *Mepe* expression. To check the Dlx5 binding affinity for the putative homeodomain response elements, we made probes for H1, H2, and H3 as h1, h2, and h3 WT and mutant (MT) forms (Fig. 5*E*) and then we determined the Dlx5 binding affinity by EMSA (Fig. 5*D*). We incubated the radiolabeled h1, h2, and h3 WT and MT probes with *in vitro* transcribed-translated Dlx5 proteins and found a remarkable difference in the Dlx5 binding affinity for each of the three putative response elements (data not shown). To compare the specific binding affinity to the Dlx5 protein, we made a radiolabeled h2 WT probe, which bound in a complex with the Dlx5 protein (Fig. 5*D*, *lane 3* and *arrowhead*), and then we competed the binding of Dlx5 to radiolabeled h2 WT probe with a molar excess of cold h1 (Fig. 5*D*, *lanes 4–6*), h2 (Fig. 5*D*, *lanes 7–9*), and h3 (Fig. 5*D*, *lanes 10–12*) WT probes. The h2 MT probe did not show specific binding to the Dlx5 protein (Fig. 5, *D*, *lane 13*, mutant probe designated *E*). The HA-tagged Dlx5-DNA probe complex was supershifted with anti-HA antibody (Fig. 5*D*, *lane 14* and *asterisk*). Our EMSA data indicated that the binding affinity to Dlx5 was highest in h2 WT and lowest in the h1 WT probe. Because H1 is not conserved in the rat *Mepe* promoter and it has the lowest binding affinity, we ruled out H1 as a candidate for the Dlx5 response element. In the experiment with mutant constructs, the basal level and fold-induction by Dlx5 with M-253 were lower than with M-147 in the ROS 17/2.8 cells (Fig. 5*F*). To analyze the binding ability of H2 and H3 to Dlx5 *in vivo*, we performed a ChIP assay (Fig. 5*G*).

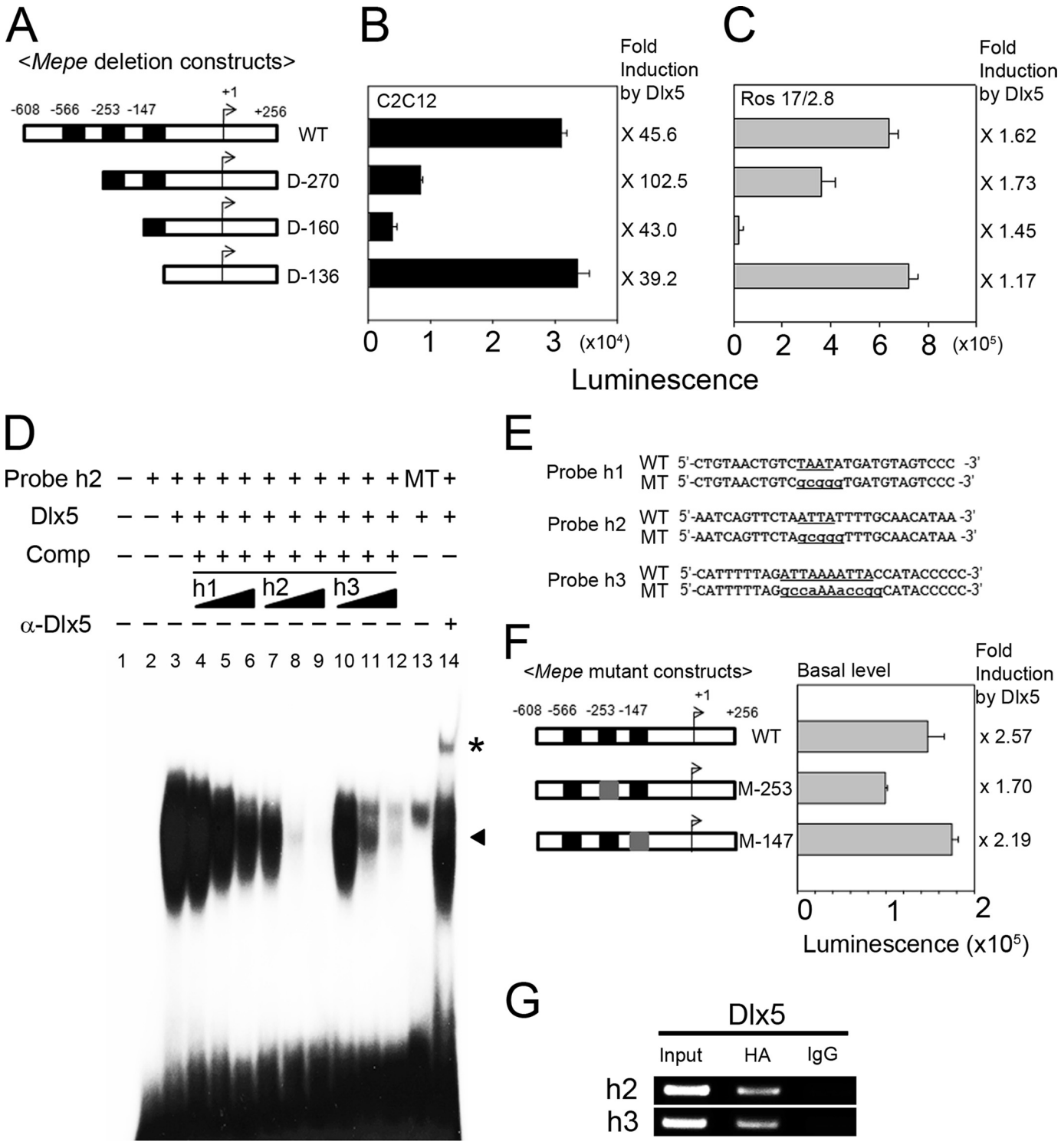

FIGURE 5. **Putative homeodomain response elements in the *Mepe* promoter are specifically activated by Dlx5.** *A*, *Mepe* promoter serial deletion constructs are illustrated in *A*. *B* and *C*, C2C12 cells and ROS 17/2.8 cells were transfected with *Mepe* promoter WT and 5′ serial deletion constructs (D-270, D-160, and D-136) with a pcDNA3.1 empty vector for the basal level and Dlx5 expression vector. Luciferase activities are expressed as the mean ± S.E. for triplicates. *D*, ^{32}P-labeled h2 probe was incubated with *in vitro* transcribed-translated HA-Dlx5 protein. *Lane 1*, mock; *lane 2*, free probe; *lanes 3–12*, Dlx5 protein incubated with the labeled h2, probe alone (*lane 3*), or in the presence of a 10-, 50-, or 100-fold molar excess of unlabeled h1, h2, or h3 oligonucleotides (*lanes 4–6*, *7–9*, and *10–12*, respectively); *lane 13*, h2 mutant probe; *lane 14*, Dlx5 binding confirmed by a supershift assay with anti-HA antibody. The *arrowhead* indicates binding of Dlx5 to each probe, and the *asterisk* indicates a supershift by anti-HA antibody. *E*, the *Mepe* promoter construct bearing three putative homeodomain response elements between −608 and +256 bp was subjected to making probes for EMSA (probes h1, h2, and h3 WT and MT), and site-directed mutagenesis for H2 and H3 to substitute the ATTA or TAAT sequences with the designated sequences in *E*. *F*, *Mepe* promoter mutant constructs are illustrated in *F*. C2C12 cells were transfected by electroporation with *Mepe* promoter mutant constructs (*M-253* and *M-147*) and pcDNA3.1 empty vector or Dlx5 expression vector. Luciferase activities are expressed as the mean ± S.E. for triplicates. *G*, ChIP assays were performed with MC3T3-E1 cells transiently transfected with HA-Dlx5 by electroporation. Anti-HA antibody mediated the precipitation of chromatin fragments PCR-amplified with primers for h2 and h3, which are listed in Table 3.

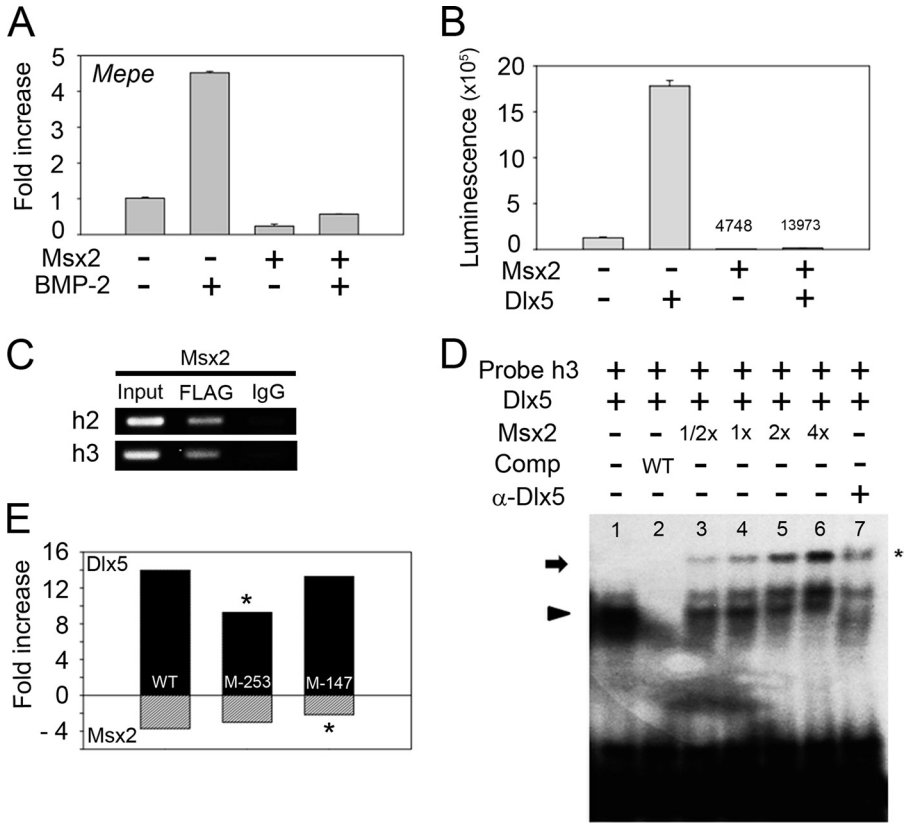

FIGURE 6. **Dlx5 and Msx2 are competing for common response elements**. *A*, mock-transfected MC3T3-E1 cells and MC3T3-E1 cells that were stably transfected by electroporation with Msx2 were treated with BMP-2 (100 ng/ml) for 1 day after reaching visual confluence, and *Mepe* expression was determined by quantitative real time PCR. The relative levels of *Mepe* mRNA were normalized to those of *Gapdh*. *B*, C2C12 cells were transiently cotransfected with the *Mepe* promoter construct (WT) and Dlx5 and/or Msx2 expression vectors. *C*, ChIP assays were performed with MC3T3-E1 cells transiently transfected with FLAG-Msx2 by electroporation. Anti-FLAG antibody was used to precipitate chromatin fragments PCR-amplified with primers for h2 and h3, which are listed in Table 3. *D*, binding to the Dlx5 protein with radiolabeled h3 probe was competed against Msx2 protein. Each protein was transcribed-translated *in vitro*. The h3 probe was incubated with a fixed Dlx5 protein. *Lane 1*, major binding complex with HA-Dlx5 was competed by a 100-fold molar excess of unlabeled h3 competitor (*lane 2*). *Lanes 3–6*, the binding complex with Dlx5 (*arrowhead*) gradually formed after addition of increasing amounts of Msx2 (*arrow*). *Lane 7*, the *asterisk* indicates a supershift by anti-HA antibody against HA-Dlx5. *E*, C2C12 cells were transiently cotransfected with *Mepe* promoter mutant constructs (*M-253* and *M-147*) and Dlx5 and/or Msx2 expression vectors. Luciferase activities were determined based on triplicates per each experiment and three independent experiments and normalized to the basal level with empty vector expression.

Msx2 Antagonizes the Regulatory Effect of Dlx5 on Mepe Expression by Competing Common Response Sites—Our previous report noted that Dlx5 stimulates *Alp* expression, but Msx2 antagonizes the stimulatory effect of Dlx5 (22). Based on this finding, we proposed that Msx2 suppresses *Mepe* expression like it suppresses BMP-2-induced *Alp* expression. Msx2 overexpression in MC3T3-E1 cells suppresses *Mepe* expression with or without BMP-2 (Fig. 6*A*). To support the antagonizing effect of Msx2 on *Mepe* expression, we transfected the Dlx5 and/or Msx2 expression vectors with the *Mepe* promoter (WT) reporter vector together in C2C12 cells (Fig. 6*B*). *Mepe* promoter activity was increased by Dlx5 and decreased by Msx2, and Dlx5-stimulated promoter activity was completely suppressed by Msx2. Moreover, ChIP assay data indicates that Msx2 also bind to H2 and H3 *in vivo* (Fig. 6*C*). Based on these observations, we supposed that Msx2 recognizes the common homeodomain response elements that are occupied by Dlx5. To examine the Msx2 binding affinity, we performed EMSA with the labeled h2 and h3 WT probes. Our previous observation indicated that the binding affinities of h2 and h3 for Dlx5 were higher, so we ruled out the h1 probe and incubated h2 and h3 WT probes with a constant amount of Dlx5 protein and an increasing amount (× 1/2, 1, 2, and 4) of Msx2 protein (Fig. 6*D*). With increasing amounts of Msx2 protein, only the h3 WT probe showed an increased h3 WT probe-Msx2 binding complex (Fig. 6*D*, *arrow*) and decreased h3 WT probe-Dlx5 complex (Fig. 6*D*, *arrowhead*). Incubation of the h2 WT probe with Dlx5 and/or Msx2 in the same manner showed only a slight increase in the h2 WT-Msx2 complex and a small decrease in h2 WT-Dlx5 complex bands with increasing Msx2 (data not shown). Dlx5-h3 WT complex bands disappeared with unlabeled h3 WT probe (Fig. 6*D lane 2*), and a supershift confirmed that the binding complex included Dlx5 (Fig. 6*D*, *lane 7*). Bands between the *arrow* and *arrowhead* (Fig. 6*D*) were confirmed as nonspecific bands, which did not disappear with the Mut probe (Fig. 5*D*, *lane 13*). Luciferase assay with mutant constructs for H1 (M-253) and H2 (M-147) showed that an increase by Dlx5 overexpression was significantly decreased in M-253-transfected cells and suppression by Msx2 overexpression was significantly diminished in M-147-transfected cells (Fig. 6*E*). Taken together, we suggest that Msx2 antagonizes the Dlx5 stimulatory effect by competing for common homeodomain response elements but has binding priority at H3 in the *Mepe* promoter.

Runx2 Stimulates Mepe Expression—In the *MEPE* promoter sequence alignment, two highly conserved Runx2 response elements were found in human, mouse, and rat (Fig. 4*A*). However, *Mepe* expression and its promoter reporter activity regulation by Runx2 overexpression were lower than those by Dlx5 overexpression (Figs. 3, *B* and *D*, and 4*C*). To determine the binding pattern of Runx2, we made individual Runx2 binding element mutant constructs, M-165 and M-127 for R1 and R2, respectively. In the luciferase reporter assay with mutant constructs in C2C12 cells, M-165 showed the lowest activity basal level and fold-induction by Runx2 (Fig. 7*A*). Based on this result, we proposed that R1 has a stronger Runx2 binding affinity than R2. In the absence of Dlx5 in C2C12 cells, *Mepe* was not expressed (Fig. 2*C*), but *Mepe* was still expressed in Runx2$^{-/-}$ cells in which Dlx5 was expressed (Fig. 7*B*). In a luciferase reporter assay using Runx2$^{-/-}$ cells, Dlx5 and/or Runx2 overexpression

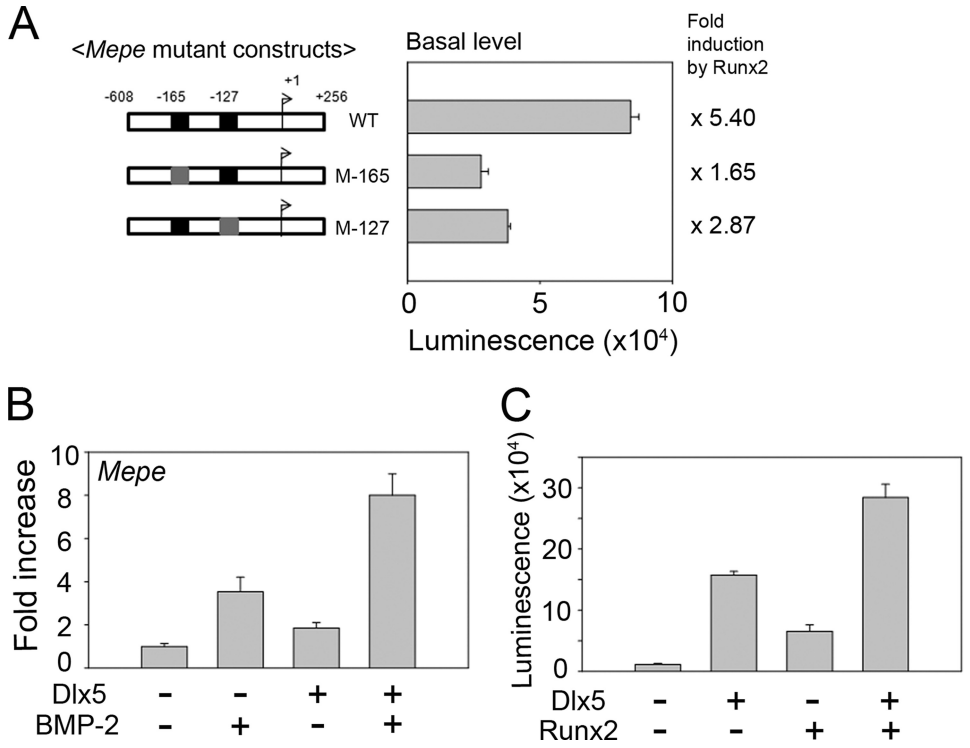

FIGURE 7. **Runx2 stimulates *Mepe* expression.** *A*, C2C12 cells were transiently cotransfected with *Mepe* promoter mutant constructs (*M-165* or *M-127*) and pcDNA 3.1 empty vector or Runx2 expression vector. *B*, mock-transfected Runx2$^{-/-}$ cells and Runx2$^{-/-}$ cells that were stably transfected by electroporation with Runx2 treated with or without BMP-2 (100 ng/ml) for 1 day after reaching visual confluence, *Mepe* expression was determined by quantitative real time PCR. The relative levels of *Mepe* mRNA were normalized to those of glyceraldehyde-3-phosphate dehydrogenase (*Gapdh*). *C*, Runx2$^{-/-}$ cells were transiently cotransfected with the *Mepe* promoter construct and Dlx5 and/or Msx2 expression vectors. *A* and *C*, luciferase activities are expressed as the mean ± S.E. for triplicates from three independent experiments.

increased reporter activity in the same manner as in C2C12 and ROS 17/2.8 cells (Fig. 7*C*). Taken together, Dlx5 is an indispensable component of the transcriptional machinery that up-regulates *Mepe* expression. Furthermore, Dlx5 acts independently of Runx2, with the role of Runx2 in *Mepe* expression being significant, but less important, than the role of Dlx5.

DISCUSSION

MEPE is widely known to be a specific marker of osteoblasts and osteocytes and a modulator of body phosphate metabolism. It is one of the SIBLING family proteins (osteopontin, bone sialoprotein, dentin matrix protein 1, dentin sialophosphoprotein, and MEPE) (10), for which the transcriptional regulation mechanisms are relatively well understood, except for MEPE (14). In this study, we uncovered how *MEPE* gene expression is regulated by BMP-2 and BMP-2 downstream osteogenic transcriptions factors such as Dlx3, Dlx5, Runx2, Osx, and Msx2.

Mepe Expression Is Bone Cell-specific—It is well known that *Mepe* expression is highly specific for bone tissue. *In vitro*, *Mepe* is expressed in differentiated osteoblasts, with notably increased expression during osteoblast-mediated matrix mineralization (23, 24). Our previous study (16) showed that *Bmp-2* expression is coordinated with *Dlx5* and *Runx2-II* expression in mouse calvarial bone development. Moreover, Dlx5 is specifically expressed in osteoblast cells and is a direct and specific target of BMP-2 signaling (17). In this paper, *Mepe* was specifically expressed and induced by BMP-2 in osteogenic cells in which Dlx5 is expressed (Fig. 2*C*). Also, *Mepe* expression can be stimulated by Runx2, but Runx2 is not a major regulator of *Mepe* expression, because *Mepe* is expressed and induced by Dlx5 overexpression or BMP-2 treatment in Runx2$^{-/-}$ cells (Fig. 7*B*). In the case of non-osteogenic C2C12 cells in which Dlx5 expression is not detected (25), we were unable to detect *Mepe* cDNA amplification even after 40 cycles of real time PCR. *Mepe* expression in C2C12 cells, as represented by the C_t value, was finally detected 3 days after BMP-2 treatment. However, the level was still much lower (1/10–1/30) than the basal *Mepe* mRNA level in MC3T3-E1 cells (Fig. 2*C*). This observation shows that C2C12 cells become committed to an osteogenic fate as a result of BMP-2 treatment and acquire osteogenic character with *Mepe* expression. Our results indicate that *Mepe* expression induced by BMP-2 is more closely related to *Dlx5* gene expression than to any other osteogenic transcription factor. *Mepe* expression is basally detected in Dlx5-positive cells, but is not detectable in Dlx5-negative cells.

Demonstration of Gene Expression Levels during Osteoblast Differentiation Using the "Relative ΔCt Value"—In this paper, we introduced the concept of relative ΔCt value (Fig. 1*B*, 2, B and C). We subtracted the individual ΔCt value from the highest ΔCt value (1 day ΔCt value of *Mepe* in our data (ΔCt value = gene Ct value − *Gapdh* Ct value)). Because the ΔCt value is inversely related to the gene expression level (high ΔCt value indicates low gene expression and low ΔCt value indicates high gene expression), we tried to design the value to positively correlate with the expression level. Usually, the fold-value expressed as the ΔΔCt value power of 2 ($2^{\Delta\Delta Ct\ value}$) to show gene expression is the same with the difference of relative ΔCt value power of 2 ($2^{difference\ of\ relative\ \Delta Ct\ value}$) in this relative ΔCt value concept. Because the fold-value for *Mepe* expression shows a big gap (about 2^{18}) between days 1 and 21 in our data, we needed a way to show *Mepe* expression levels with other gene expression levels clearly in a graph. Thus, the relative ΔCt value is a convenient way to express thousand- or million-fold differences in single gene expression levels during cell differentiation. Moreover, it is also useful to be able to simultaneously compare the relative expression levels of multiple genes.

Mepe Expression Is Strongly Stimulated by BMP-2 Treatment and Activation of Downstream Molecules in the BMP-2 Signaling Pathway—BMP-2 is a potent cytokine in osteoblast differentiation and it induces osteogenic transcription factors, Dlx3, Dlx5 and Runx2-II (16, 22, 25). Our results indicate that *Mepe*

expression is specifically regulated by BMP-2 treatment (Fig. 2*A*). Consistently, *Mepe* expression was also stimulated by Dlx3, Dlx5, and Runx2-II overexpression (Fig. 3, *B* and *D*, and supplemental Fig. S3) and suppressed by siDlx3 (supplemental Fig. S3), siSmad1/5, siDlx5 (Fig. 3, *A* and *C*), Msx2 (Fig. 6, *A* and *B*), and siRunx2 (Fig. 3*E*). These observations suggest that *Mepe* expression is one target of the BMP-2 signaling pathway. Msx2 is believed to antagonize Dlx5 activity by repressing activity at the promoter of various osteogenic markers, including osteocalcin (26), bone sialoprotein (27), α1(I) collagen (28), and ALP (22). Two mechanisms have been proposed to explain how Msx2 counteracts Dlx5. In one model, both factors compete for the same binding site in the target promoters (29, 30). Alternatively, interactions between Msx2 and Dlx5 homeodomains may inhibit Dlx5 binding to the target promoters (31). In this paper, our EMSA data supports the former idea, with Dlx5 and Msx2 competing for the same homeodomain response elements in the *Mepe* promoter (Fig. 6*D*). In addition, we found that Dlx5 and Msx2 commonly bind to the same region, however, they have a different binding specificity to H2 and H3, respectively. In the ChIP assay, we could check that Dlx5 and Msx2 bind to H2 and H3 *in vivo* (Figs. 5*G* and 6*C*), however, we could not confirm the binding priority to the H2 and H3, because they are so closely located (about 100 bp; Fig. 4*A*) that our ChIP assay could not discriminate binding priorities between the two elements. In the EMSA assay and mutagenesis for H2 and H3, Dlx5 showed higher specificity for the H2 element, whereas Msx2 had a higher specificity for H3 (Figs. 5*D* and 6, *D* and *E*). In contrast, another BMP-2 downstream transcription factor, Osx, does not have a significant role in regulating *Mepe* expression. Osx overexpression in MC3T3-E1 cells marginally suppressed *Mepe* expression (supplemental Fig. S4). Although both Dlx5 and Runx2 act as positive regulators and have an additive effect on *Mepe* expression, Dlx5 activity is critical for *Mepe* expression; *Mepe* expression is not detected in the absence of Dlx5 (Fig. 2*C*), but is detected in Runx2$^{-/-}$ cells (Fig. 7*B*). Moreover, Dlx5 overexpression induced higher *Mepe* expression than Runx2 overexpression (Figs. 3, *B* and *D*, and 4*C*). Although, Dlx5 is the most potent mediator to *Mepe* expression, BMP-2 treatment with siDlx5 increased *Mepe* expression somewhat (Fig. 3*C*). We suppose that there might be another pathway to regulate *Mepe* expression instead of BMP-2. The β-catenin in the canonical Wnt signaling pathway is a candidate, because we found LEF-1 response elements in the *Mepe* promoter sequence, and there have been some reports concerning cross-talks between BMP-2 and Wnt signal transduction (32, 33).

Role of MEPE in Osteoblast Differentiation—There is controversy surrounding the exact roles of MEPE in biomineralization. It is widely known that MEPE acts as a bone mineralization inhibitor (minhibin) and phosphate uptake inhibitor (phosphatonin) in renal proximal tubules (6). These actions are mediated by the ASARM motif, which is supported by the finding of increased bone mineral density in the *Mepe* knock-out mouse (12) and the dose-dependent hypophosphatemia observed in mice treated with intraperitoneal injection of MEPE (3). In contrast, MEPE has been shown to have an anabolic effect on osteoblast differentiation. It is reported that AC-100 enhances osteogenesis by promoting osteoblast proliferation and differentiation like BMP-2 (8, 9). Dentonin, which is the same as AC-100, promotes dental pulp stem cell proliferation in response to the dentin repair response (34, 35). Furthermore, *Bmp-2, Dlx5*, and *Mepe* expressions are increased during healing of a bone fracture (36). Our data suggest that BMP-2-induced *Mepe* and *Phex* expression are much higher in the early differentiation stage than in the late differentiation stage (Fig. 2*B*). We assumed that MEPE is protected by PHEX, which is also induced by BMP-2 and may have an anabolic property in the early differentiation stage of osteogenesis, much like AC-100. However, the activity of AC-100, which is a synthetic 23-amino acid peptide, does not fully represent MEPE function. PHEX is a known inhibitor of the ASARM peptide release by cathesin B. However, a recent report (37) also suggests that PHEX degrades the circulating phospho-ASARM peptide, which inhibits matrix mineralization. During normal matrix mineralization *in vitro*, treatment of MC3T3-E1 cells with exogenous PHEX alone does not result in a significant increase in mineralization and PHEX rescues mineralization inhibition when exogenous phospho-ASARM is present (37). Collectively, we contend that when the PHEX level is greater than the MEPE level, MEPE is protected from cathepsin B cleavage action by PHEX. Even if ASARM is present, it is degraded by PHEX and then MEPE shows an osteogenic action in the proliferation and matrix maturation stage. However, when the PHEX level is lower than the MEPE level, the ASARM peptide is actively cleaved and released by cathepsin B, allowing it to protect osteocytes and odontoblasts from burial by mineralization. In conclusion, we show that *MEPE* expression is specifically regulated by BMP-2 signaling and that this regulation is mediated by Dlx5 and Msx2 proteins and homeodomain response elements of the *MEPE* promoter, with different binding priorities. Furthermore, *PHEX,* as well as *MEPE* expression is up-regulated by BMP-2, and transcriptional and protein levels of *MEPE* and *PHEX* are inversely related to the osteoblast differentiation and mineralization stages in MC3T3-E1 cell long-term cultures. The *in vitro* data presented here suggest that *MEPE* transcriptional regulation as well as the balance between MEPE and PHEX activities are important for bone mineralization associated with bone fracture or bone disease.

REFERENCES

1. Econs, M. J., McEnery, P. T., Lennon, F., and Speer, M. C. (1997) *J. Clin. Invest.* **100,** 2653–2657
2. White, K. E., Carn, G., Lorenz-Depiereux, B., Benet-Pages, A., Strom, T. M., and Econs, M. J. (2001) *Kidney Int.* **60,** 2079–2086
3. Rowe, P. S., Kumagai, Y., Gutierrez, G., Garrett, I. R., Blacher, R., Rosen, D., Cundy, J., Navvab, S., Chen, D., Drezner, M. K., Quarles, L. D., and Mundy, G. R. (2004) *Bone* **34,** 303–319
4. Rowe, P. S. (2004) *Crit. Rev. Oral Biol. Med.* **15,** 264–281
5. Rowe, P. S., de Zoysa, P. A., Dong, R., Wang, H. R., White, K. E., Econs, M. J., and Oudet, C. L. (2000) *Genomics* **67,** 54–68
6. Quarles, L. D. (2003) *Am. J. Physiol.* **285,** E1–E9
7. Ogbureke, K. U., and Fisher, L. W. (2005) *Kidney Int.* **68,** 155–166
8. Nagel, D. E., Khosla, S., Sanyal, A., Rosen, D. M., Kumagai, Y., and Riggs, B. L. (2004) *J. Cell. Biochem.* **93,** 1107–1114
9. Sprowson, A. P., McCaskie, A. W., and Birch, M. A. (2008) *J. Orthop. Res.* **26,** 1256–1262
10. Qin, C., Baba, O., and Butler, W. T. (2004) *Crit. Rev. Oral Biol. Med.* **15,** 126–136

11. White, K. E., Larsson, T. E., and Econs, M. J. (2006) *Endocr. Rev.* **27,** 221–241
12. Gowen, L. C., Petersen, D. N., Mansolf, A. L., Qi, H., Stock, J. L., Tkalcevic, G. T., Simmons, H. A., Crawford, D. T., Chidsey-Frink, K. L., Ke, H. Z., McNeish, J. D., and Brown, T. A. (2003) *J. Biol. Chem.* **278,** 1998–2007
13. Martin, A., David, V., Fisher, L., Hedge, A., and Rowe, P. (2007) *J. Bone Miner. Res.* (*abstr.*) **22,** F1118
14. Bellahcène, A., Castronovo, V., Ogbureke, K. U., Fisher, L. W., and Fedarko, N. S. (2008) *Nat. Rev. Cancer* **8,** 212–226
15. Cho, J. Y., Lee, W. B., Kim, H. J., Mi Woo, K., Baek, J. H., Choi, J. Y., Hur, C. G., and Ryoo, H. M. (2006) *Gene* **372,** 71–81
16. Lee, M. H., Kim, Y. J., Yoon, W. J., Kim, J. I., Kim, B. G., Hwang, Y. S., Wozney, J. M., Chi, X. Z., Bae, S. C., Choi, K. Y., Cho, J. Y., Choi, J. Y., and Ryoo, H. M. (2005) *J. Biol. Chem.* **280,** 35579–35587
17. Lee, M. H., Kim, Y. J., Kim, H. J., Park, H. D., Kang, A. R., Kyung, H. M., Sung, J. H., Wozney, J. M., Kim, H. J., and Ryoo, H. M. (2003) *J. Biol. Chem.* **278,** 34387–34394
18. Choi, J. Y., Lee, B. H., Song, K. B., Park, R. W., Kim, I. S., Sohn, K. Y., Jo, J. S., and Ryoo, H. M. (1996) *J. Cell. Biochem.* **61,** 609–618
19. Choi, K. Y., Kim, H. J., Lee, M. H., Kwon, T. G., Nah, H. D., Furuichi, T., Komori, T., Nam, S. H., Kim, Y. J., Kim, H. J., and Ryoo, H. M. (2005) *Dev. Dyn.* **233,** 115–121
20. Yoon, W. J., Cho, Y. D., Cho, K. H., Woo, K. M., Baek, J. H., Cho, J. Y., Kim, G. S., and Ryoo, H. M. (2008) *J. Biol. Chem.* **283,** 32751–32761
21. Urist, M. R. (1965) *Science* **150,** 893–899
22. Kim, Y. J., Lee, M. H., Wozney, J. M., Cho, J. Y., and Ryoo, H. M. (2004) *J. Biol. Chem.* **279,** 50773–50780
23. Petersen, D. N., Tkalcevic, G. T., Mansolf, A. L., Rivera-Gonzalez, R., and Brown, T. A. (2000) *J. Biol. Chem.* **275,** 36172–36180
24. Argiro, L., Desbarats, M., Glorieux, F. H., and Ecarot, B. (2001) *Genomics* **74,** 342–351
25. Lee, M. H., Kwon, T. G., Park, H. S., Wozney, J. M., and Ryoo, H. M. (2003) *Biochem. Biophys. Res. Commun.* **309,** 689–694
26. Newberry, E. P., Latifi, T., and Towler, D. A. (1998) *Biochemistry* **37,** 16360–16368
27. Barnes, G. L., Javed, A., Waller, S. M., Kamal, M. H., Hebert, K. E., Hassan, M. Q., Bellahcene, A., Van Wijnen, A. J., Young, M. F., Lian, J. B., Stein, G. S., and Gerstenfeld, L. C. (2003) *Cancer Res.* **63,** 2631–2637
28. Dodig, M., Kronenberg, M. S., Bedalov, A., Kream, B. E., Gronowicz, G., Clark, S. H., Mack, K., Liu, Y. H., Maxon, R., Pan, Z. Z., Upholt, W. B., Rowe, D. W., and Lichtler, A. C. (1996) *J. Biol. Chem.* **271,** 16422–16429
29. Hoffmann, H. M., Catron, K. M., van Wijnen, A. J., McCabe, L. R., Lian, J. B., Stein, G. S., and Stein, J. L. (1994) *Proc. Natl. Acad. Sci. U.S.A.* **91,** 12887–12891
30. Ryoo, H. M., Hoffmann, H. M., Beumer, T., Frenkel, B., Towler, D. A., Stein, G. S., Stein, J. L., van Wijnen, A. J., and Lian, J. B. (1997) *Mol. Endocrinol.* **11,** 1681–1694
31. Zhang, H., Hu, G., Wang, H., Sciavolino, P., Iler, N., Shen, M. M., and Abate-Shen, C. (1997) *Mol. Cell. Biol.* **17,** 2920–2932
32. Rawadi, G., Vayssière, B., Dunn, F., Baron, R., and Roman-Roman, S. (2003) *J. Bone Miner. Res.* **18,** 1842–1853
33. Chen, Y., Whetstone, H. C., Youn, A., Nadesan, P., Chow, E. C., Lin, A. C., and Alman, B. A. (2007) *J. Biol. Chem.* **282,** 526–533
34. Liu, H., Li, W., Gao, C., Kumagai, Y., Blacher, R. W., and DenBesten, P. K. (2004) *J. Dent. Res.* **83,** 496–499
35. Six, N., Septier, D., Chaussain-Miller, C., Blacher, R., DenBesten, P., and Goldberg, M. (2007) *J. Dent. Res.* **86,** 780–785
36. Niikura, T., Hak, D. J., and Reddi, A. H. (2006) *J. Orthop. Res.* **24,** 1463–1471
37. Addison, W. N., Nakano, Y., Loisel, T., Crine, P., and McKee, M. D. (2008) *J. Bone Miner Res.* **23,** 1638–1649